Chapter 3

Effect of thermomechanical processing on mechanical properties and microstructural evolution of Al-Mg-Zn alloy

3.1 Introduction

This study investigates the impact of thermomechanical processing route on the microstructural evolution, and mechanical properties (tensile strength, hardness and elastic plastic (J_{1c}) fracture toughness) of the 7075-aluminum alloy. As received 7075 Al Alloy underwent for the solution heat treatment (SHT) followed by artificial aging and cold rolling (CR) process, respectively. Generally, it was observed that cold rolling of 7075 Al alloy is very challenging, but in this work 90 % cold rolling successfully achieved by optimizing the thermo-mechanical process. The novel heat treatment process for achieving the 90% cold rolling reduction as follow: firstly, SHT was performed at 470°C for 8 hours(h), there after aging at 140°C for 21 h was performed. Characterization techniques like X-ray diffraction (XRD), optical microscopy (OM), scanning electron microscopy (SEM), transmission electron microscopy (TEM) was employed to assess the microstructure and phase constituents. Elastic plastic (J_{1c}) fracture toughness was studied well on SHT, peak aged and rolled sample. Additionally, Vickers hardness and tensile test were performed. Aging and Cold rolling treatment effectively enhanced tensile strength and hardness ascribed to formation of fine rod shape precipitates of η"(Mg_2Zn_3) and formation of sub grains with localized strain accumulation, respectively. Split diffraction spots with satellite pattern in long range ordering has also observed in selected area electron diffraction (SAED) pattern of η" attributable to stacking faults and periodic arrangement of precipitates, respectively, as

a consequence of this 90% cold rolling of 7075 Al alloy was accomplished. The maximum Vickers hardness, Tensile strength and Elastic plastic (J_{1c}) fracture toughness values were achieved after SHT (470°C for 8 h), peak aged (PA) (140°C for 21 h) and 90% cold rolling are 226 HV, 526 MPa and 344.54 kJ/m^2, respectively.

3.2Materials Characterization

3.2.1 Xray Diffraction

Xray diffraction is performed to verify the solution heat treatment process and aging process. At first XRD of as received sample is performed which is shown in Fig.3.1 (a) (red color graph), peaks of Al are coming at 38.4955, 44.3085, 65.260 and 78.426 degrees and peaks of precipitates are showing in between of 38.4955 and 44.3085 degrees. Firstly, solution heat treatment is performed at 470°C for 2 hours, but the precipitates are not dissolved fully in Al matrix as the peaks of precipitates can be seen clearly in XRD graph of Fig. 3.1 (a) (blue color graph), like XRD of as received sample. Again, SHT is performed at 470°C for 4 hours and 3.1 hours, their XRD are represented in yellow and green color graph of Fig. 3.1(a) respectively. When XRD is performed at 470°C for 8 hours, all precipitates are dissolved in matrix and only the peaks of Al are observed in XRD graph like Fig. 3.1 (a) (violet color graph) which ensures material is successfully solution heat treated. XRD of peak aged sample is also performed to ensure the formation of precipitates which can be clearly seen in Fig. 3.1 (b). The XRD pattern for SHT is showing a single-phase aluminum structure, typically face-centered cubic (FCC), as aluminum is an FCC metal, because all precipitates dissolved during SHT process (Fig. 3.1 (a) violet color XRD graph). Solution heat treatment is optimized and perfect time and temperature are achieved which is at 470°C for 8 hours

During aging, the alloying elements precipitate from the solid solution and form various precipitate phases. Diffraction peaks corresponding to the newly formed precipitate phases can be seen XRD graph of aged sample (Fig. 3.1(b)). From fig 3.1(b) it's clear that very fine precipitates of Mg_2Zn_3 are formed, because broad peak of Mg_2Zn_3 is detected between 38.4955- and 44.3085-degrees Al peaks, which is showing nano size precipitation has taken place [31,34,89,90].

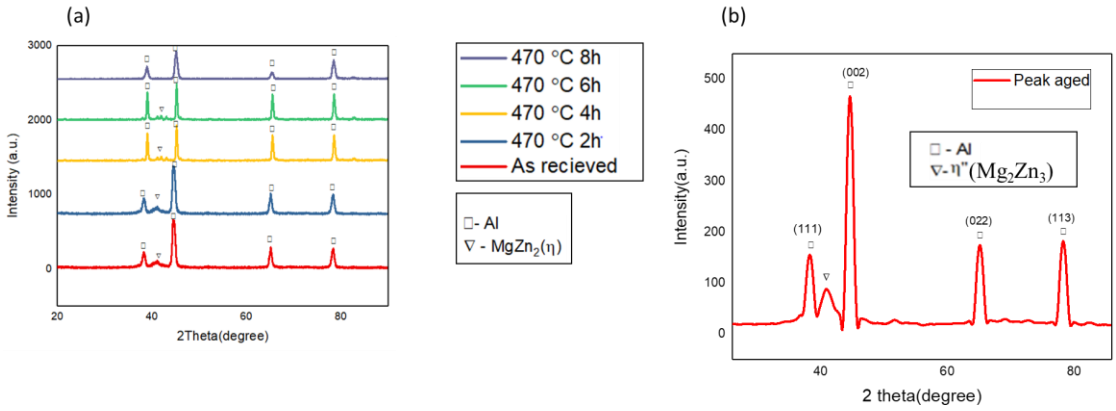

Fig. 3.1: (a) XRD of as received (red color graph), SHT at 470°C for 2 hours (blue color graph), SHT at 470°C for 4 and 6 hours (yellow and green color graph), SHT at 470°C for 8 hours (violet color graph), (b) XRD of peak aged sample.

Mg_2Zn_3 is metastable precipitate of 7075 Al alloy at peak aged condition (fig 3.1(b)), while $MgZn_2$ is stable precipitate of as received 7075 Al alloy at over aged condition (red colour graph of Fig. 3.1(b)).

3.2.2 Microstructure investigation

Optical image of SHT shown in Fig. 3.2(a) is clarifying that precipitates are dissolved in matrix and larger grain boundary is showing due to dissolution of all precipitates (quenching "freezes" the solute atoms in the solid solution, preventing them from precipitating [28]). In SHT condition there were no precipitates on grain boundary.

Grain size is calculated with the assistance of ImageJ analysis and found average grain size of 51 µm. Microstructure in an aged 7075 Al alloy, the formation of small, evenly distributed precipitates on the grain boundary can be observed clearly. These precipitates are quite small and are dispersed uniformly throughout the microstructure. Fig. 7(b) is the microscopy image of 21 hours aged sample in which no. of grain boundaries are increasing and size of grains are decreasing. Average grain size of peak aged sample is decreased up to 21 µm at peak aged condition. Fig 3.2(c) is the zoomed image of fig 3.2(b) in which formation of fine precipitates and dispersoids can be clearly seen on grain boundary.

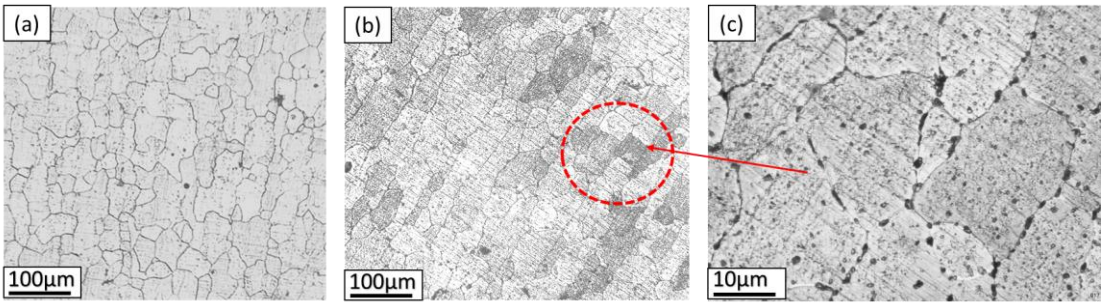

Fig. 3.2: (a) Optical image of SHT sample (470°C for 8 h), (b) Optical image of peak aged (SHT+PA) sample (140°C for 21 h), (c) optical image of peak aged sample at higher magnification

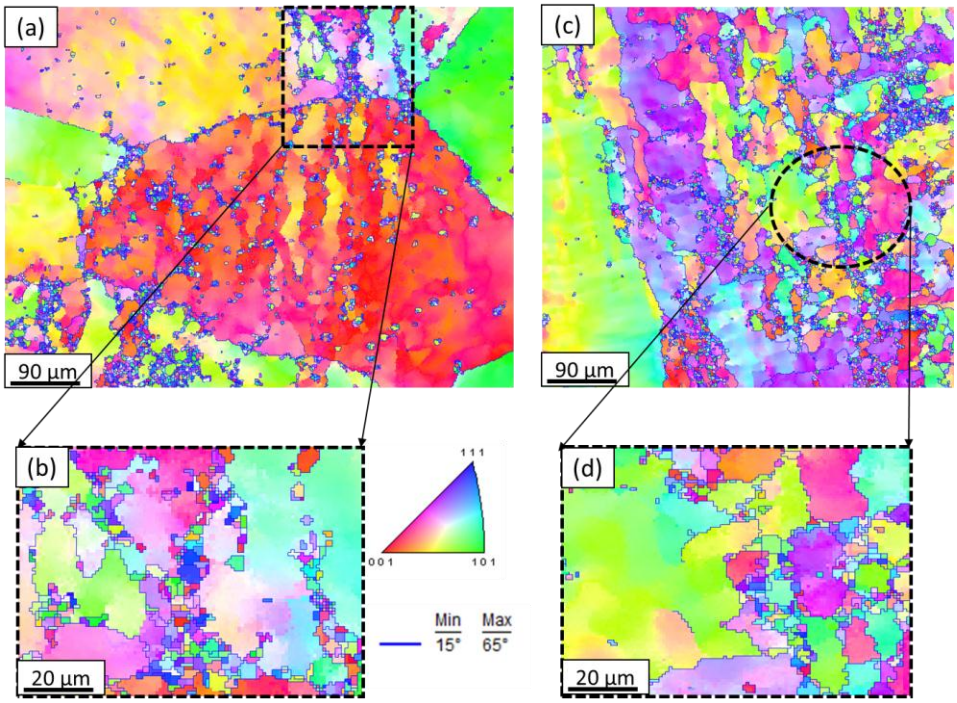

Fig 3.3 (a, b) IPF image of 45% cold rolled sample after SHT and (c, d) IPF image of 90% cold rolled sample (SHT+PA+90% CR) after peak aged

From the Inverse pole figure Maps (Fig. 3.3), it is evident that the volume fraction of sub-grains in the 45% cold-rolled sample is lower compared to the 90% cold-rolled sample. This difference is attributed to the lower distortion energy during the 45% cold rolling process. In the 90% cold-rolled sample, the higher distortion energy accelerates dynamic recovery and recrystallization [28,29]. In both the 45% and 90% cold-rolled samples (Fig.3.3), stable grains are formed due to the presence of high-angle grain boundaries [30, 31] Additionally, sub-grains of varying sizes (<1 µm) are formed during both the 45% and 90% cold rolling processes.

3.2.3 Transmission Electron Microscopy

The transmission electron microscopy analysis of the peak aged displays a predominantly fine and evenly dispersed precipitation within the grains, as depicted in Fig. 3.4 (a, b, c). Moreover, the precipitates at the grain boundaries appear finer and

more closely spaced. Rod like morphology of η" precipitate is noticed which is clearly shown in Fig. 3.4(d). In the case of the SAED patterns from the peak aged, numerous spots correspond to the metastable precipitate of η" is represented (Fig. 3.4 (e)). To understand the SAED pattern clearly a dummy image (Fig. 3.4 (f)) of SAED pattern is drawn which is showing a characteristic pattern of split diffraction spots with satellite pattern in long range ordering. White spots are corresponded to the matrix while small satellite green spots are corresponding to η". The composition of the η" precipitate is found Mg_2Zn_3. For peak-aged 7075 aluminum alloy, SAED pattern is showing a well-defined diffraction pattern corresponding to the crystallographic planes of the aluminum matrix and the precipitate phases.

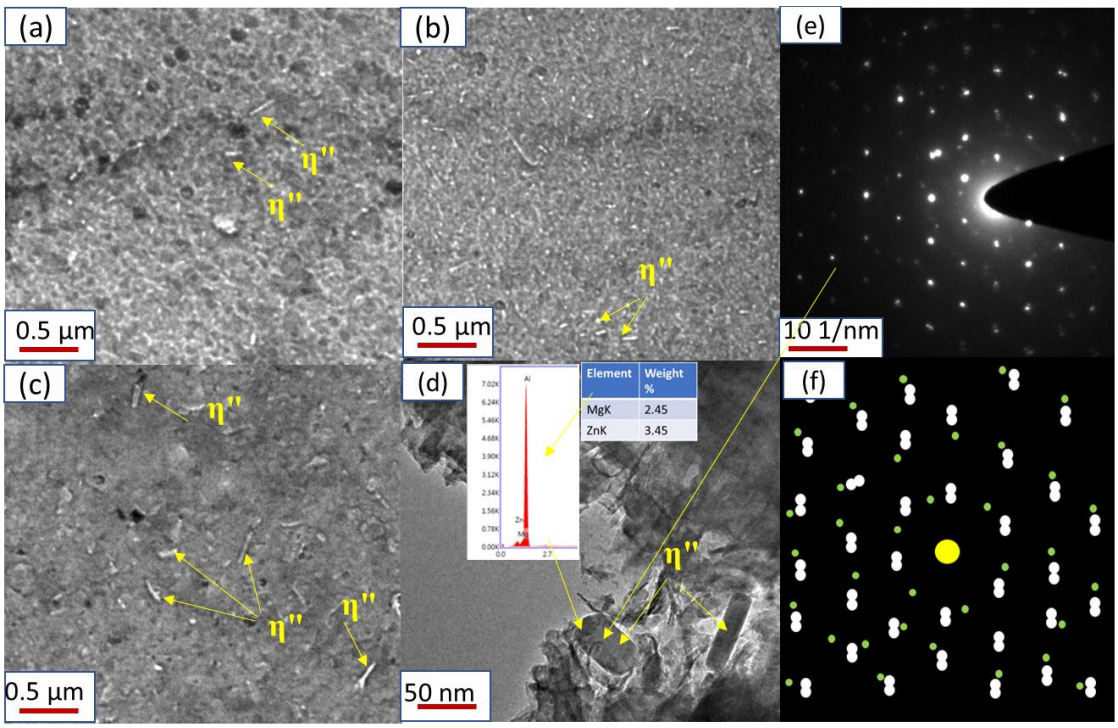

Fig. 3.4: (a), (b) and (c) is the TEM image of peak aged sample, (d) is zoomed image of η" precipitate, (e) is the SAED pattern of η" particle highlighted in image (d), (f) is dummy image of SAED pattern in which satellite pattern with long range ordering can be seen very clearly.

Mechanical Characterization

3.3.1 Hardness test

Hardness test is conducted to find the hardness of solution heat treated, aged and rolled sample. Vickers hardness machine is used for this purpose. At 140°C aging process, hardness of solution heat treated sample is about 128 HV and for peak aged process hardness was observed at 21 hours is 195 HV. After peak aging due to Ostwald ripening precipitates are getting coarser[24] and hardness value is decreasing from 195 HV to 143 HV. Hardness of rolled samples is observed 226.5 HV which is the highest hardness observed compared to all investigated condition.

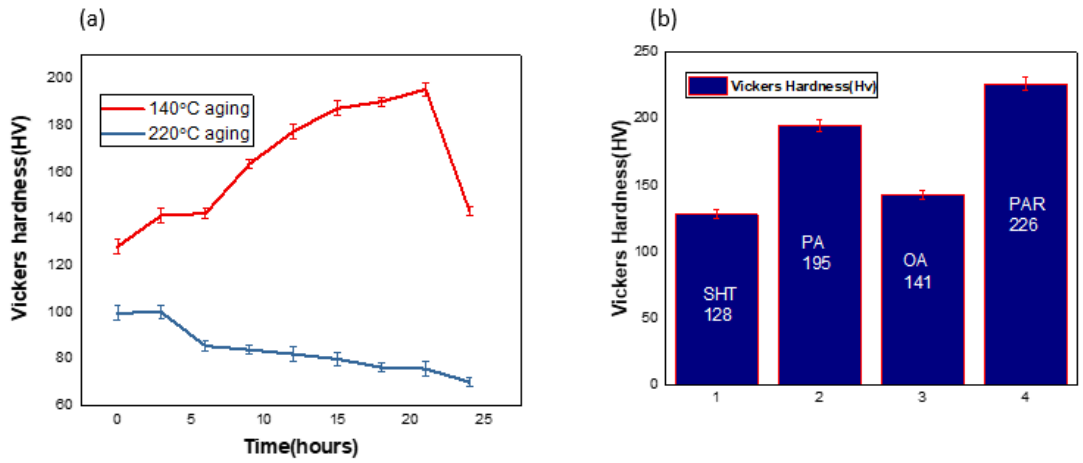

Fig. 3.5: (a) Hardness graph of SHT+140°C aging (red color graph) and SHT+220°C (blue color graph), (b) hardness graph of (1) SHT at 470°C 8 h, (2) (PA) Peak aging at 140°C 21 h, (3) (OA) Over aging at 140°C 24 h 24 h (4) Peak Aged at140°C 21 h and 90% cold rolled (PAR)

3.3.2 Tensile test

Tensile test was performed to find the yield stress, the ultimate tensile strength and the percentage elongation of the sample. The UTS of as received, SHT, peak aged, peak aged and 90% cold rolled samples are 462.8± 5 MPa, 280± 10 MPa, 496.5±10

MPa and 526±5 MPa, respectively was obtained. The Yield stress of as received, SHT, peak aged, peak aged and rolled samples are 375.837±5 MPa, 150± 10 MPa, 450±10 MPa and 480± 5MPa, respectively, was obtained. The average elongation of as received, SHT, peak aged, peak aged and rolled samples are 11±1 %, 12 ±2 %, 8 ±3% and 6±2%, respectively. Fig. 3.6 is showing the tensile test graph for as received (AR), SHT, peak aged (SHT+PA) and 90% cold rolled (SHT+PA+90% CR) sample

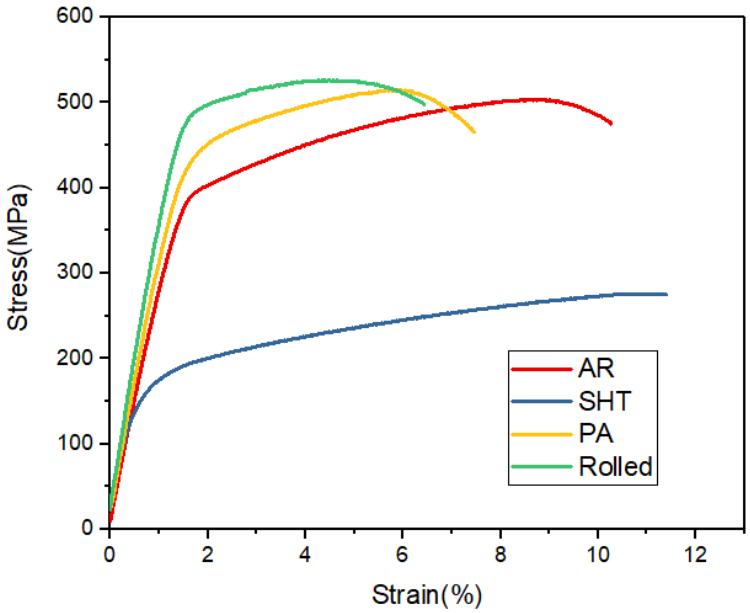

Fig. 3.6: Tensile test graph for as received (AR), SHT, peak aged (SHT+PA) and 90% cold rolled (SHT+PA+90% CR) sample

3.3.3 Elastic plastic (J_{1c}) fracture toughness

(J_{1c}) fracture toughness of 7075 Al alloy at SHT, peak aged and 90% cold rolled conditions are determined. Load vs displacement graph is studied well and compared for all three conditions. The load vs. displacement curve for a (J1c) fracture toughness of SHT, peak aged (SHT+PA) and 90% rolled (SHT+PA+90%CR) samples are shown in fig 3.7. The fracture toughness under plane stress conditions was determined using

the LPD (load point displacement) Load curve theory, as specified by the equation provided in ASTM E1820-13[95] .

$$J = \frac{K^2(1-\vartheta^2)}{E} + J_{pl} \tag{3.1}$$

where

$$k = \frac{P}{T_N W} \frac{\left(2+\frac{a}{w}\right)[0.886+4.64\left(\frac{a}{w}\right)-13.32(\frac{a}{w})^2+14.72(\frac{a}{w})^3-5.6(\frac{a}{w})^4}{(1-\frac{a}{w})^{(\frac{3}{2})}} \tag{3.2}$$

and

$$J_{pl} = \frac{n_{pl} A_{pl}}{T_N b} \tag{3.3}$$

Equations (3.1)–(3.3) define A_{pl} as the region under the LPD-Load curve from the origin to the maximum load, illustrated in Fig. 3.7. TN represents the net specimen thickness (TN = T, the sample thickness, in the absence of side grooves). W corresponds to the sample width, K represents the stress intensity factor, v denotes the Poisson ratio, E designate the Young modulus of rigidity, a indicates the crack length, and b signifies the uncrack ligament determined by

b =(W-a)

and

$$n_{pl} = 2 + 0.522\frac{b}{W} \tag{3.4}$$

For the Al alloys, the values are E = 70 GPa and v = 0.33. For the rolled sample, the η_{pl} value (derived from Eq. (3.4)) is 3.753, and Apl is determined as 8970 N-mm (according to Fig. 3.7(c)). Subsequently, employing Eq. (3.1), J_{pl} is computed to be 320.54 kJ/m^2, and using Eq. (3.4), the value of K is assessed as 456.624 N/mm^2. Plugging these K and J_{pl} values into Eq. (3.1) yields an average plane stress fracture toughness of 344.54$\pm$10 kJ/m^2 for the rolled sample. Analogously, the average plane

stress fracture toughness values for SHT and peak aged (SHT+PA) samples are identified as 82.5±5 kJ/m2, 230.35±7 respectively.

To confirm if the fracture toughness calculated via LPD-Load curve theory aligns with the valid fracture toughness (J_{IC}), certain conditions regarding the specimen need to be fulfilled [27].

$$b \geq \frac{25J_{1c}}{\sigma_f} \tag{3.5}$$

$$B \geq \frac{25J_{1c}}{\sigma_f} \tag{3.6}$$

When assessing elastic plastic fracture toughness, parameters like the sample thickness (B), yield strength (σf), and elastic plastic fracture toughness (J_{IC}) are used. In this study, the values of elastic plastic fracture toughness (344.54 kJ/m2) and yield strength (483 MPa) were applied to equations (5) and (6) to validate the elastic plastic fracture toughness. The minimum unbroken ligament (b) and thickness (B) necessary to confirm the elastic plastic fracture toughness were found to be 17.394 mm for rolled, 16.34 mm for aged and 13.5 mm for SHT samples.

However, the sample thickness used in the present study was 5.7 mm, with an unbroken ligament of 25.4 mm. This revealed that the derived "B" values for the rolled, SHT and peak aged samples did not fulfill the requirement stated in Eq. (3.6). Consequently, due to the failure to satisfy both thickness criteria, the calculated plane stress fracture toughness for rolled, SHT and aged samples represents a conditional fracture toughness (J_Q).

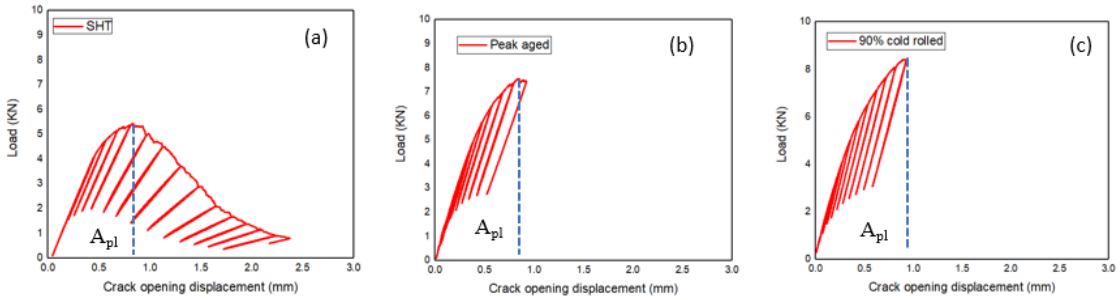

Fig. 3.7: Load vs displacement diagram of (a) SHT, (b) Peak aged, (c) Peak aged and 90% cold rolled samples (SHT+PA+90% CR)

3.4 Fractography

Fig. 3.8 (a, b) is showing fractography image of SHT samples in which big size of ductile dimples and voids are observed in large numbers, which was indicating ductile fracture [96]. Fig.3.8 (c, d) is indicating fractography image of peak aged sample in which some small size ductile dimples and voids with cleavage facets are perceived. The fracture surface in the aged condition is showing a combination of ductile and brittle fractures with dimples, trans granular cracking and inter granular cracking [97]. Fig.3.8 (e, f) is fractography image of the 90% cold rolled (SHT+PA+90%CR) sample, exhibit prevalence of cleavage facets, beach mark, and river like pattern. The existence of brittle fractures can be attributed to the grain refinement and work hardening processes [97,98].

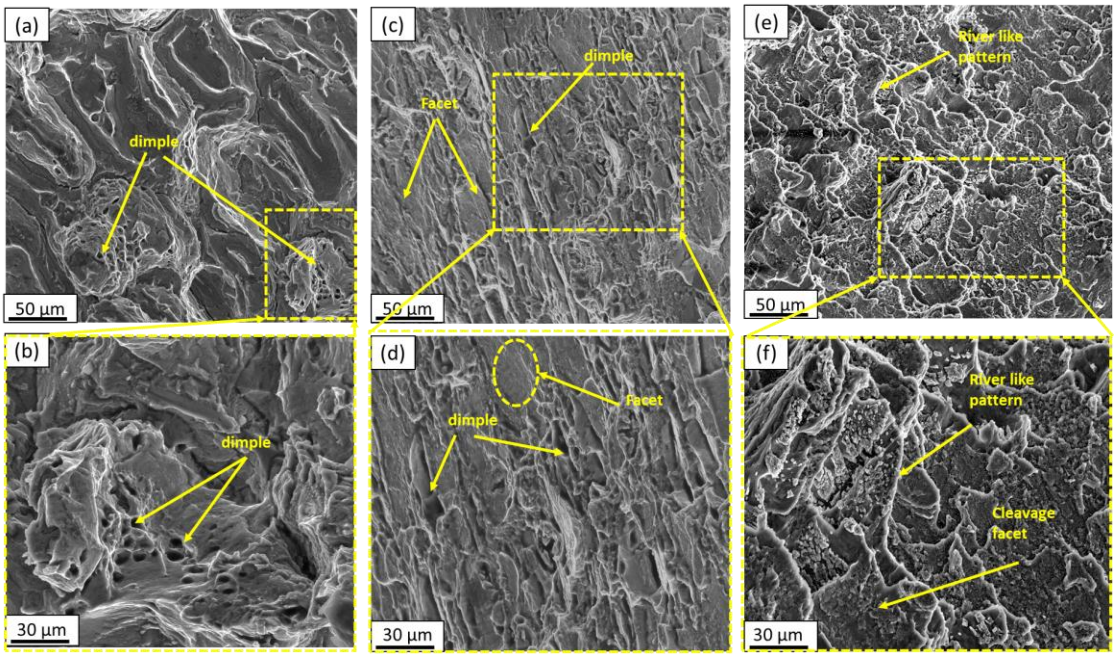

Fig. 3.8: Fractography image of SHT (a, b), peak aged (c, d), 90% cold rolled samples (SHT+PA+90% CR) (e, f) after tensile test

In aluminum alloys like 7075, the fracture mode is often a combination of ductile and brittle fracture. The presence of dimples, micro voids, or tearing indicates ductile fracture, while cleavage facets suggest brittle fracture [99]. Fig. 3.9 showing the fractography image of CT samples in SHT, aged and 90% cold rolled condition respectively and supporting the tensile fracture result as well. Micro voids and ductile dimples are noticed in SHT sample, while ductile dimple with cleavage facet is remarked in peak aged sample, and river like pattern is perceived in 90% cold rolled (SHT+PA+90%CR) sample.

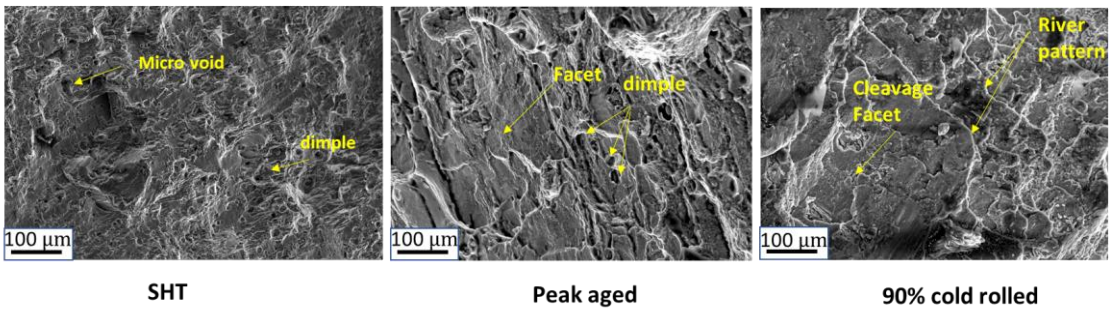

Fig. 3.9: Fractography of CT sample in SHT, peak aged (140°C 21H) and 90% cold rolled (SHT+PA+90% CR) condition.

3.5 Discussion

3.5.1 Microstructural and Mechanical properties correlation

The grains are relatively larger in the case of SHT which can be clearly observed in Fig. 3.2(a), where no precipitates were formed on the grain boundaries and within the grains, attributable to dissolution of all precipitates [90]. However, during the subsequent aging step, the precipitation of fine particles within the material takes place. As the precipitation process continues during aging, the grain boundaries act as nucleation sites for these precipitates [100]. This leads to the formation of fine precipitate particles along the grain boundaries, and within the grains [37]. The presence of these fine precipitates impedes the growth of aluminum grains[44,85], preventing them from reaching larger sizes during the aging process. Consequently, the grain size of the alloy decreases as a result of the precipitation hardening [28,101], which can be remarked clearly in Fig. 3.2(c). In the present work fine precipitates of η" (Mg_2Zn_3) is observed at peak aging condition which is confirmed by XRD (Fig. 3.1(b)), TEM (Fig. 3.4 (a), (b), (c) and (d)) and SAED (Fig. 3.4 (e), (f)) pattern analysis. These η" fine precipitates hinder the movement of dislocations [16,102,103]. Therefore, hardness and tensile strength of peak aged sample is more than SHT sample, and that is the one reason for

fracture surfaces in SHT condition are showing larger ductile dimples and voids formation (fig 3.9(a, b)), responsible for ductile fracture[104], whereas fracture surface of aged sample is showing relatively smaller dimples, and formation of micro voids with regions of flat, trans-granular cleavage with distinctive facets (Fig.3.9(c, d)). This suggests a mix mode of ductile and brittle failure mechanisms[105,106]. At 220°C aging hardness is decreasing after 3 hours because at high temperature nucleation is less and growth rate is higher[107]. After 21 hours (over aging), due to Ostwald ripening process [29], agglomeration of the precipitates[27] is started and coarsening of grains also occurred simultaneously. The higher hardness value and tensile strength of 90% cold rolled sample was noticed because of severely deformation of grains and formation of nano-size sub grains due to localized strain accumulation [108–110] due to cold rolling, which can be clearly observed in IPF image of 90% cold rolled sample in Fig. 3.3(b). Fracture surfaces of cold rolled condition was depending on the degree of rolling and the orientation of the sample. The cleavage facet, beach mark and river like pattern was observed on the fracture surface of 90% (SHT+PA+ 90%CR) samples, indicating brittle fracture [111–113]. These features indicate plastic deformation and slip along the crystal planes due to the rolling process. Split diffraction spot in SAED (Fig. 3.4 (e) and (f)) is might be due to formation of stacking fault[114]. Stacking faults introduce local changes in the crystal structure, affecting the diffraction pattern and causing spot splitting [115].

3.5.2 Mechanism behind achieving 90% cold rolling

Artificial aging involves reheating the material to a lower temperature to allow the precipitation [116]. In the present work with the help of SAED pattern of peak aged sample (Fig. 3.4 (e) and 3.4 (f)), it was confirmed that η" is prevailed in Al matrix in a

periodic manner with long range ordering. Alloy with well-ordered precipitates may exhibit improved formability and workability due to its enhanced strength and structure [117,118]. The satellite pattern and split diffraction spots (Fig. 3.4 (f)) suggest a controlled microstructure [119]. Split spots are observed due to stacking faults[12,120], which indicate the improvement in the deformability[121]. Therefore, after artificial aging, the material has become less prone to cracking during deformation processes during cold rolling. This is the reason for 90% cold rolling is successfully achieved in 7075 Al alloy after peak aging process which can be clearly seen in Fig. 2.9(d) and 1(e). In SHT condition precipitates dissolve fully and make super saturated solid solution [122]. The cold rolling process after solution heat treatment is difficult due to the absence of stacking faults and periodic arrangement of precipitates[123]. This makes the material more susceptible for cracking during cold rolling as can be observed in Fig. 2.9 (a), 2.9 (b) and 2.9(c).